BIOINFORMATION
Discovery at the interface of physical and biological sciences

open access www.bioinformation.net Hypothesis

Volume 9(8)

Binding mode prediction of biologically active compounds from plant *Salvia Miltiorrhiza* as integrase inhibitor

Nadtanet Nunthaboot[1]*, Kiattisak Lugsanangarm[2], Sirirat Kokpol[2] & Ibrahim S Abd-Elazem[3]

[1]Department of Chemistry and Center of Excellence for Innovation in Chemistry, Faculty of Science, Mahasarakham University, Mahasarakham,44150, Thailand; [2]Department of Chemistry, Faculty of Science, Chulalongkorn University, Bangkok, 10330, Thailand; [3]Department of Biology, The Johns Hopkins University, Baltimore, Maryland, 21218, USA; Nadtanet Nunthaboot - Email: nadtanet@gmail.com; *Corresponding author

Received March 30, 2013; Accepted April 01, 2013; Published April 30, 2013

Abstract:
Integrase (IN), an essential enzyme for HIV-1 replication, has been targeted in antiretroviral drug therapy. The emergence of HIV-1 variants clinically resistant to antiretroviral agents has lead to the development of alternative IN inhibitors. In the present work, binding modes of a high potent IN inhibitor, $M_5$22 and $M_5$32, within the catalytic binding site of wild type (WT) IN were determined using molecular docking calculation. Both $M_5$22 and $M_5$32 displayed similar modes of binding within the IN putative binding pocket and exhibited favorable interactions with the catalytic Mg^{2+} ions, the nearby amino acids and viral DNA through metal-ligand chelation, hydrogen bonding and π-π stacking interactions. Furthermore, the modes of action of these two compounds against the mutated Y212R, N224H and S217H PFV IN were also predicted. Although the replacement of amino acid could somehow disturb inhibitor binding mode, almost key interactions which detected in the WT complexes were fairly conserved. Detailed information could highlight the application of $M_5$22 and $M_5$32 as candidate IN inhibitors for drug development against drug resistant strains.

Keywords: Integrase, Docking, Drug resistance, Mutation.

Background:
Acquired immunodeficiency syndrome (AIDS), caused by human immunodeficiency virus (HIV), is an epidemic worldwide serious health disease. Currently, a highly active antiretroviral therapy (HAART), which consists of drugs targeting reverse transcriptase (RT) and protease (PR) enzymes, is used for the treatment of HIV-1 infection. However, the limitation of RT and PR inhibitors in terms of side effects and drug resistance leads to an effort to develop new drugs to be a third component of HAART. HIV-1 integrase (IN), one of the three important enzymes in HIV life cycle, has become an attractive target for AIDS therapy. Due to no known similar enzyme in human, therefore, specific HIV-1 IN inhibitor is expected to have minimal side effects compared to other antiviral agents. HIV-1 IN is composed of three distinct domains, N-terminal (residues 1-50), catalytic core (residues 50-212), and C-terminal (residues 212-288). The N-terminal domain is involved in enzyme multimerization while the C-terminal domain has strong but nonspecific DNA-binding activity and thus has been called the DNA-binding domain. Catalytic residues, Asp64, Asp116, and Glu152, are located in the central core domain and coordinate with the divalent metal cation, either Mg^{2+} or Mn^{2+}. Although the structures of each individual or the two fragment domains were obtained by X-ray crystallography and nuclear magnetic resonance (NMR) spectroscopy **[1-3],** there is no experimentally completed structure of HIV-1 IN. HIV-1 IN catalyzes two well characterized reactions referred to a terminal 3′-end processing

(the cleavage of two terminal nucleotides from the 3′-ends of viral double-stranded DNA) and a strand transfer (joining of the processed 3′-ends of the virus to the 5′-phosphate groups in the human chromosomal DNA). In addition, IN is capable of catalyzing the reverse reaction referred to a disintegration process.

A currently most promising HIV-1 IN inhibitor is the diketo acids (DKAs) which inhibit the strand transfer reaction. The bifunctional DKA derivatives were found to bind both the acceptor host DNA and the viral donor DNA sites of IN and inhibit both 3′-processing and strand transfer mechanisms **[4]**. Although DKAs were found to be effective against viral integration in infected cells, this class of inhibitors leads to drug-induced mutations in HIV-1 IN **[5]**. Currently, raltegravir, a strand transfer inhibitor, is the only approved IN inhibitor **[6]**. However, the resistance of this commercial drug has been reported **[7, 8]**. There are three primary mutations for raltegravir resistance. The two primary resistance pathways involved mutations of the amino acids at Q148 (Q148K/R/H) or N155 (N155/H) whereas a third primary mutation pathway at Y143 (Y143C/R) was less commonly found **[9, 10]**. The secondary mutation at position G140 (G140S) combined with primary mutation Q148K/R/H significantly enhanced drug resistance. Indeed, the occurrence of drug resistance is a major reason for the failure of antiretroviral therapies in HIV-1 infection **[7, 8]**. Therefore, it is necessary to continue seeking HIV-1 IN inhibitors with high potency that are non-toxic and inhibit drug-resistant strains.

The bottleneck of structure-based design of HIV-1 IN has been complicated due to a lack of co-crystallized structure of ligand with isolated protein or with the DNA complex. Although the only experimentally resolved X-ray crystal structure of the HIV-1 IN complexed with 1-(5-chloroindol-3-yl)-3-hydroxy-3-(2H-tetrazol-5-yl)-propenone (5CITEP) inhibitor was available, it was believed that the bound conformation of ligand was influenced by crystal packing effect **[1]**. Recently, crystal structures of full-length IN protein from prototype foamy virus (PFV) complexed with viral DNA and two Mg^{2+} ions were solved with raltegravir **[10]**. The intasome structure provided further an understanding of binding orientation of IN strand transfer inhibitor. The carbonyl and hydroxyl groups of both compounds were observed to directly chelate the catalytic metal ions while the halobenzyl moiety displaced the reactive 3′-hydroxy group of viral DNA end by 6 Å relative to the free ligand bound IN active site **[10]**. The PFV IN intasome could be considered as a model to develop HIV-1 IN strand transfer inhibitors as suggested by the docking studies **[11, 12]** as it could provide an understanding of the binding modes of HIV-1 IN strand transfer inhibitors. In the preset work, molecular docking calculations were performed on the two highly potent and non-toxic HIV-1 IN inhibitors, lithospermic acid ($M_5$22) and lithospermic acid B ($M_5$32) extracted from the roots of the Danshen plant *Salvia miltiorrhiza* **[13]**. These two polyphenolic compounds inhibited both 3'end processing and strand transfer with IC_{50} values in the range of 0.37-0.83 µM and strongly suppressed acute HIV-1 infection in H9 cells (IC_{50} of 2-6.9 µM) and were not cytotoxic at high concentrations (CC_{100}>297 µM and 223 µM, respectively. Binding orientations and favorable interactions of ligands against the wild-type (WT) and three different mutation strains; Y212R (equivalent to Y143R HIV-1 IN), N224H (equivalent to N155H HIV-1 IN) and S217H (equivalent to G140S/Q148H HIV-1 IN) of PFV IN were predicted.

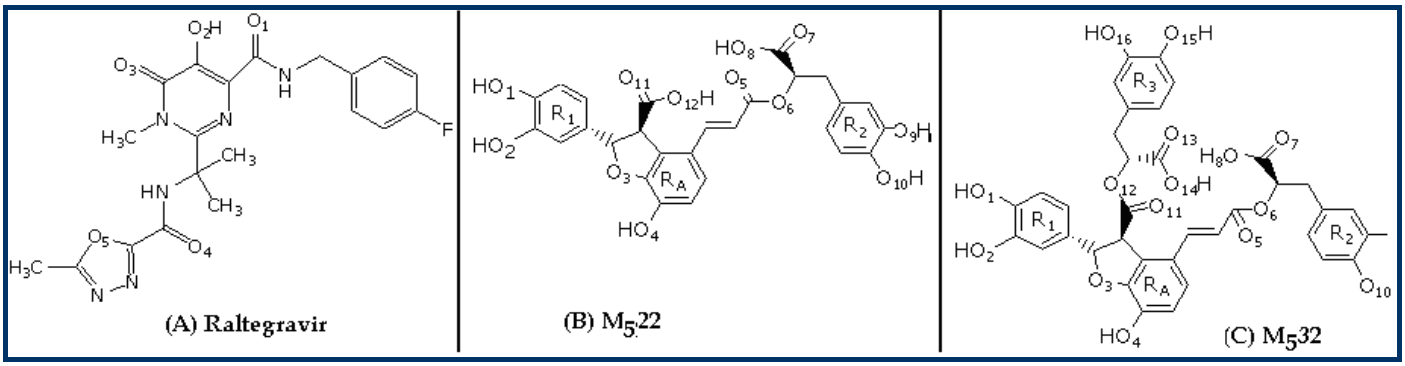

Figure 1: Chemical structure and atomic numbering of **(A)** Raltegravir; **(B)** $M_5$22 and **(C)** $M_5$32**.**

Methodology:

Protein preparation

The X-ray crystal structures of WT, N224H (corresponding to N155H HIV-1 IN) and S217H (corresponding to G140S/Q148H HIV-1 IN) PFV IN/DNA intasome retrieved from Protein Data Bank with pdb code 3OYA, 3OYN, and 3OYL, respectively, were used for docking study **[10]**. The structure corresponding to Y143R mutation of HIV-1 IN was obtained by modifying the WT structure of PFV IN bound to raltegravir (3OYA). Tyrosine at position 212 was replaced by amino acid arginine. The proteins were initially prepared by removing the coordinates of ligand and water molecules. Hydrogen atoms were added and the CHARMM force field was subsequently applied to optimize the protein structure.

Ligand Preparation

The structures of the $M_5$22 and $M_5$32 **(Figure 1)** were built and geometry optimized at the semi-empirical PM6 level of theory using the MOPAC2009 program **[14]**.

Molecular Docking

Molecular docking calculations were carried out using CDOCKER module implemented in Discovery studio 2.0 **[15]**. The binding pocket of the native co-crystallized ligand was identified as the protein active site. The docking calculations were performed using the default settings. The receptor was held rigid while the rotatable bonds of ligand were allowed to rotate during the calculation. Docking procedures were validated by docking the native raltegravir into the active site of

the PFV IN and then the docked conformations were compared to that of X-ray complex structure (see supplementary material). Both $M_5$22 and $M_5$32 compounds were consequently docked into the active site of WT and mutated IN intasome by using the same procedures as raltegravir.

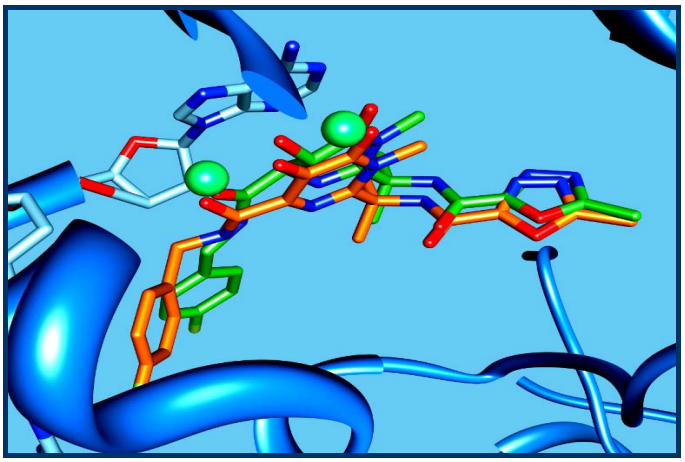

Figure 2: Comparison the orientation of X-ray (orange) and the docked (green) conformer of raltegravir. The X-ray conformer is taken from Protein Data Bank (PDB code: 3OYA) [1] to [10]. The docking result shows the RMSD value of 1.31 Å while the key interactions are conserved.

Discussion:

Validation of Docking Protocol

To validate the computational docking protocol, raltegravir was extracted and docked back to its corresponding binding pocket. The best docking pose could reproduce the optimal orientation and position of raltegravir to be close to that of its original orientation detected in the X-ray complex structure **(Figure 2).**

Interaction mode with WT strain

The calculated binding energies of both compounds are within the same range **Table 1 (see supplementary material)** and support their comparable inhibitory potency **[13]**. The binding conformations of $M_5$22 and $M_5$32 in the binding pocket of WT PFV IN are depicted in (**Figure 3A)** while their important interactions are given in **Table 1**. Both compounds shared a similar binding pattern in which their 1st catechol moiety (R_1) chelated the two Mg^{2+} ions. In addition, the 2, 3-dihydrobenzofuran ring and one of catechol moieties (R_1) of the two ligands made π-π stacking interactions with adenosine base A17 of the viral DNA. For compound $M_5$22, the hydroxyl oxygen atoms of both catechol moieties chelated the two metal cations **(Figure 3A, left)**. Due to a steric effect, the addition of a long side chain including the 3rd catechol in compound $M_5$32, however, led to only one catechol ring (R_1) interacting with the Mg^{2+} ions **(Figure 3A, right)**. The 2nd catechol ring (R_2) of the $M_5$22 formed edge to face hydrophobic interaction with Phe190 while the six membered rings of the 2, 3-dihydrobenzofuran core structure made the hydrophobic π-π interaction with Tyr212. There was no hydrogen bond formation between IN and $M_5$22. However, this is different in the case of $M_5$32 where hydrogen bonds were found to stabilize the protein-ligand complex. One of the hydroxyl oxygen of the 2nd catechol ring (R_2) of $M_5$32 established hydrogen-bonding interaction with the backbone nitrogen of Ala188. In addition to π-π interaction with Tyr212, the 3rd catehol moiety (R_3) created hydrogen bonds with backbone nitrogen atoms of Tyr212 and His213 and carbonyl oxygen of Thr210. The addition of the 3rd catechol moiety could possibly improve the binding affinity of $M_5$32 against the WT IN through a large number of hydrogen bonding interactions.

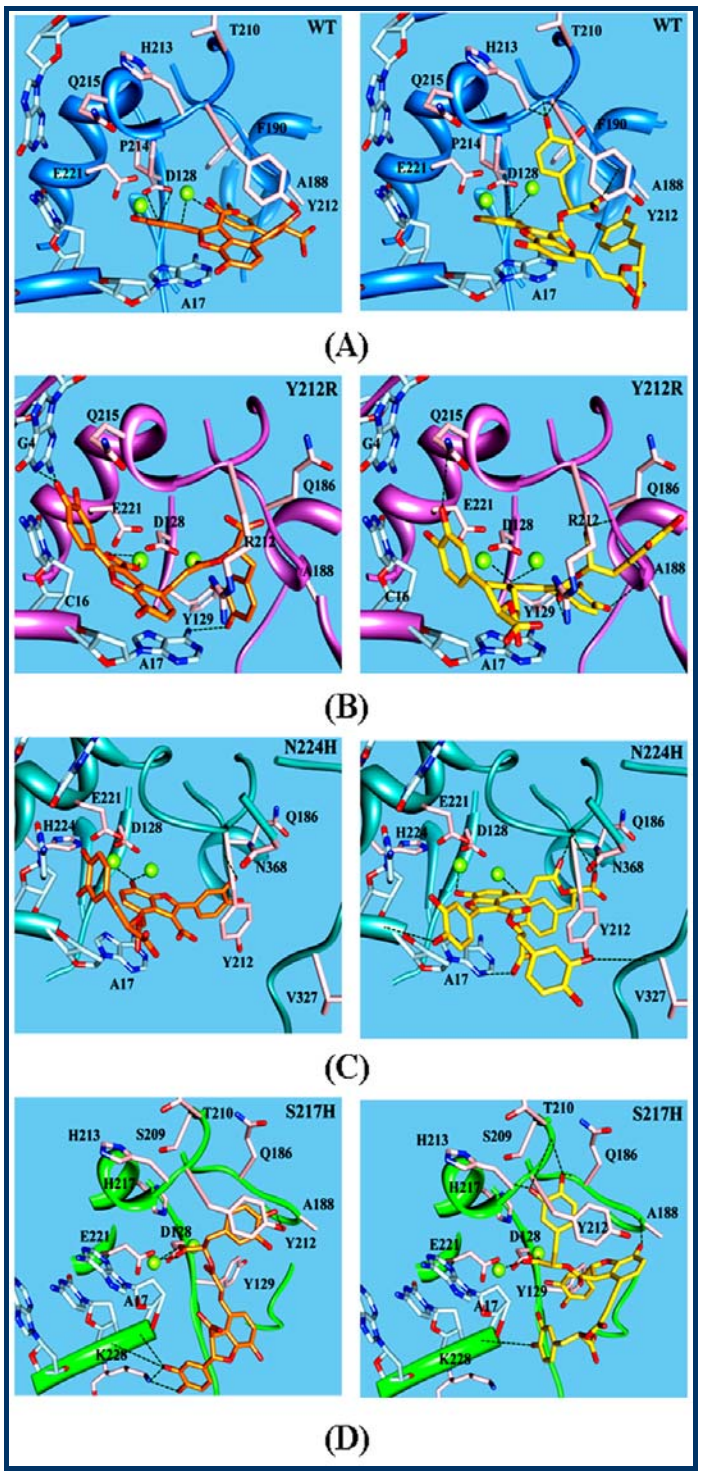

Figure 3: The docked conformations of compounds M522 (orange, left) and M532 (yellow, right) in **(A)** WT, **(B)** Y212R, **(C)** N224H and (D) S217H variants. The Mg2+ ions are in green, and hydrogen bond interactions are indicated in dashed lines. The chelation and hydrogen bond distances are given in unit of Å.

Interaction mode with the single mutation strain

The hypothetically predicted mode of action of these two

compounds against the Y212R (corresponding to Y143R HIV-1 IN) and N224H (corresponding to N155H HIV-1 IN) PFV IN are displayed in (**Figures 3B & 3C)**, respectively. Although the two compounds showed different modes of binding from those of WT complex, their binding energies were do not significantly changed (**Table 1)** except for N224H-$M_5$22 system. The proposed raltegravir resistance pathway of the less frequently Y143H/R/C has been directly related to the interaction between inhibitor and Tyr143. In the WT structure, the side chain of Tyr143 was found to form a direct π-π stacking interaction with oxadiazole ring of raltegravir, however, the replacement of Tyr by Arg (Y143R) disturbs this type of interaction, thereby could possible significantly influence drug inhibitory potency **[13, 16]**. However, from our docking calculation, although the mutation of Y212R was observed to destroy the π-π stacking interaction between protein and ligand, other types of interaction i.e. cation-π and hydrogen bond were alternatively occurred between Arg212 and $M_5$22 and $M_5$32, respectively (**Table 1)**. Hence, mutation of this particular residue may not significantly result in susceptibility of these compounds. The docking results of the N224H mutant revealed that the bound conformations of both $M_5$22 and $M_5$32 were also different from those of WT complex. The two compounds displayed similar binding pattern in which their 2, 3-dihydrobenzofuran framework pointed toward to the two divalent metal ions although their 1st catechol ring was flipped in the opposite direction **(Figure 3C).** The more stable binding interaction energy of $M_5$32 (-75.01 kcal/mol) compared to $M_5$22 (-54.58 kcal/mol) could possibly due to the stronger metal-ligand and hydrogen bonding interactions than that of $M_5$22 system. The $M_5$32 established hydrogen bonds with Tyr212, Val327, and A17 of viral DNA while this type of interaction was detected with only Gln186 in the case of $M_5$22. Our docking analysis suggested that $M_5$32 might be active against the mutation of N224H IN (corresponding to N155H HIV-1 IN).

Interaction mode with the double mutation strain

The predicted binding modes of both $M_5$22 and $M_5$32 with the S209/S217H mutant (equivalent to G140S/Q148H HIV-1 IN) are displayed in **Figure 3D.** Due to steric constraint of imidazole side chain of His, the mutation of S217H leads to inhibitor binding in another region that is different from those of WT and the other two mutant systems. Interestingly, although the binding of $M_5$22 and $M_5$32 was disturbed, they still preserved the metal-ligand chelation and some key interactions with the surrounding residues. Moreover, the two compounds shared somewhat similar modes of binding and action in which their carboxylic acid chelated the Mg^{2+} ions. The catechol moiety of both $M_5$22 and $M_5$32 interacted with viral DNA via hydrogen bond interaction with the phosphate group of A17. In addition to the carboxylic acid, the hydroxyl moiety of the 1st catechol ring of $M_5$32 was also capable to chelate one of the metal ions **(Figure 3D, right & Table 1**) while the $M_5$22 did not **(Figure 3D, left).** Again, the more stable binding interaction energy of $M_5$32 (-75.70 kcal/mol) compared to $M_5$22 (-60.97 kcal/mol) might possibly because of its stronger hydrogen bonding interactions. The $M_5$32 made hydrogen bonds with Tyr129, Gly131, Gln186, Ala188, Thr210, and His213 while hydrogen bonds between $M_5$22 and Tyr212 and Lys228 were observed. The mutation strain of G140S/Q148H in HIV-1 IN has > 150-fold reduced susceptibility to raltegravir **[16, 17]**. From our docking calculation, raltegravir lost interactions to protein; catalytic metal ion and viral DNA (see **Table 1** in supplementary material). This is different in the case of $M_5$22 and M532, Although the mutation of S217H (corresponding to G140S/Q148H of HIV-1 IN) disturbed the inhibitor binding mode, it is likely that both compounds were capable to preserve the main interactions with Mg^{2+} ions, the contacting amino acids and viral DNA. Their interaction energies were also more stable than that of raltegravir. Therefore, this mutation variant probably has relatively no influence on the key interactions between IN and both molecules in particular $M_5$32 since it could form many hydrogen bonds with the nearby amino acids.

Conclusion:

In the present work, molecular docking studies were conducted to determine the binding conformations of $M_5$22 and $M_5$32, natural compounds extracted from the Plant *Salvia Miltiorrhiza*, within the catalytic site of WT and mutation variants of PFV IN. In the WT system, the binding energies of $M_5$22 and $M_5$32 compounds were found to correspond to their comparable inhibitory potency. The most favorable finding bound conformations of these molecules directly chelated with the Mg^{2+} ions. The presence of hydrogen bonding, metal-ligand, and π-π stacking interactions plays a major role in the stabilization of the binding preference between protein and ligand. For the mutation strains, almost major interactions between ligand and amino acids of IN were fairly preserved. This study could highlight the application of $M_5$22 and $M_5$32 as candidate IN inhibitors for drug development against drug resistant strains. Development of $M_5$22 and $M_5$32 as new mutation insensitive HIV drugs for AIDS patients are currently in progress.

Acknowledgment:

This work was financially supported by the annual government statement of expenditure of Mahasarakham University (fiscal year 2011). N.N. would like to acknowledge the Center of Excellence for Innovation in Chemistry (PERCH-CIC), Office of the Higher Education Commission, Ministry of Education for financial support. Authors thank the National Nanotechnology Center (NANOTEC) for providing Discovery Studio for molecular graphics.

References:

[1] Goldgur Y *et al. Proc Natl Acad Sci USA.* 1999 **96**: 13040 [PMID: 10557269]
[2] Chen JC *et al. Proc Natl Acad Sci USA.* 2000 **97:** 8233 [PMID: 10890912]
[3] Wang JY *et al. EMBO J.* 2001 **20**: 7333 [PMCID: PMC125787]
[4] Marchand C *et al. J Biol Chem.* 2002 **227:** 12596 [PMID: 11805103]
[5] Egbertson MS, *Curr Top Med Chem.* 2007 **7:** 1251 [PMID: 17627556]
[6] Summa V *et al. J Med Chem.* 2008 **51:** 5843 [PMID: 18763751]
[7] Cooper DA *et al. N Engl J Med.* 2008 **359:** 355 [PMID: 18650513]
[8] Malet I *et al. Antimicrob Agents Chemother.* 2008 **52:** 1351 [PMID: 18227187]
[9] Métifiot M *et al. Viruses.* 2010 **2:** 1347 [PMID: 20706558]
[10] Hare S *et al. Proc Natl Acad Sci USA.* 2010 **107:** 20057 [PMID: 21030679]
[11] Billamboz M *et al. Eur J Med Chem.* 2011 **46:** 535 [PMID: 2118511]

[12] De Luca L *et al*. *Eur J Med Chem.* 2011 **46:** 756 [PMID: 21227550]
[13] Abd-Elazem IS *et al*. *Antivir Res.* 2002 **55:** 91 [PMID: 12076754]
[14] Stewart JJP, MOPAC2009. http://OpenMOPAC.net.
[15] Discovery Studio 2.0, Accelrys, Inc, San Diego, CA, 2007.
[16] Blanco JL *et al*. *J Infect Dis.* 2011 **203:** 1204 [PMID: 21459813]
[17] da Silva D *et al*. *J Antimicrob Chemother.* 2010 **65**: 1262 [PMID: 20388636]

Edited by P Kangueane
Citation: **Nunthaboot *et al.*** Bioinformation 9(8): 426-431 (2013)

BIOINFORMATION

open access

Supplementary material:

Table 1: Interaction energies and distances (Å) of hydrogen bond, metal-ligand and π-π interactions of the docked configurations of ligands.

	Systems								
	WT		Y212R (equivalent to Y143R)		N224H (equivalent to N155H)		S217H (equivalent to G140S/Q148H)		
	$M_5$22	$M_5$32	$M_5$22	$M_5$32	$M_5$22	$M_5$32	Raltegravir	$M_5$22	$M_5$32
Interaction energy (kcal/mol)	-67.12	-70.28	-67.73	-72.41	-54.58	-75.01	-45.39	-60.97	-75.70
Amino/Mg^{2+}/DNA	Ligand interacting part (type of interaction, Å)								
Asp128	-	-	-	O_4 (hb, 2.77)	-	-	-	-	-
Tyr129	-	-	-	O_4 (hb, 2.67)	-	-	-	-	O_2 (hb, 2.95)
Gly131	-	-	-	-	-	-	-	-	O_{10} (hb, 3.04)
Gln186	-	-	-	O_{14} (hb, 2.94)	O_1 (hb, 2.95)	-	-	-	O_{15} (hb, 2.94)
Ala188	-	O_9 (hb, 3.03)	-	O_1 (hb, 3.14)	-	-	-	-	O_4 (hb, 3.05)
Phe190	R_2 (π-π, 4.82)	-	-	-	-	-	-	-	-
Thr210	-	O_{15} (hb, 2.92)	-	-	-	-	-	-	O_{15} (hb,2.99) O_{16} (hb, 2.90)
Tyr212/Arg212	R_A (π-π, 4.19)	R_3 (π-π, 5.30) O_{16} (hb,3.08)	R_A (cation-π, 3.46)	O_7 (hb, 2.86) O_{11} (hb, 2.61) O_{13} (hb, 3.03)	R_1 (π-π, 4.28)	O_5 (hb, 2.95) O_8 (hb, 2.97)	-	O_9 (hb,3.25) R_2 (π-π, 4.12)	R_3 (π-π, 4.39)
His213	-	O_{15} (hb,2.92)	-	-	-	-	-	-	O_{16} (hb, 3.00)
Gln215	-	-	-	O_9 (hb,2.72)	-	-	-	-	-
Lys228	-	-	-	-	-	-	F (hb, 2.97)	O_1 (hb,2.84), O_2 (hb,2.57)	-
Val327	-	-	-	-	-	O_{15} (hb, 2.69)		-	-
Mg^{2+} (1)	O_{10} (M, 2.19) O_2 (M, 3.12)	O_2 (M, 3.22)	O_5 (M, 2.23) O_9 (M, 2.40)	O_3 (M, 1.87)	O_4 (M, 2.34)	O_9 (M, 2.23)	O_3 (M, 2.29)	O_5 (M, 2.32), O_7 (M, 2.44)	O_2 (M, 2.58) O_{13} (M, 2.29)
Mg^{2+} (2)	O_2 (M, 2.23) O_1 (M, 2.19)	O_2 (M, 2.45) O_1 (M, 2.14)	O_{11} (M, 2.39)	O_4 (M, 1.90)	O_4 (M, 2.16)	O_4 (M, 2.19)	-	O_7 (M, 3.11)	O_{13} (M, 3.92)
G4	-	-	O_1 (hb, 2.67) O_2 (hb, 2.89)	-	-	-	-	-	-
C16			R_1 (π-π, 3.69)	-	-	-	-	-	-
A17	O_2 (hb, 3.04) R_1 (π-π, 3.93)	O_1 (hb, 2.99) O_2 (hb, 3.04) R_1 (π-π, 4.34)	O_{10} (hb, 3.00) R_A (π-π, 4.22)	R_A (π-π, 4.93)	R_A (π-π, 3.72)	O_4 (hb, 2.99) O_{10} (hb, 3.12) R_A (π-π, 4.12)	-	O_2 (hb, 2.72)	O_{15} (hb,2.93)

Hb-hydrogen bond. M-metal-ligand. R_1-the 1st catechol ring; R_2-the 2nd catechol ring; R_3-the 3rd catechol ring; R_A-aromatic ring A.